Biotechnology Reports 28 (2020) e00560

Contents lists available at ScienceDirect

Biotechnology Reports

journal homepage: www.elsevier.com/locate/btre

Investigation of bioactive compounds in *Crassocephalum rubens* leaf and *in vitro* anticancer activity of its biosynthesized gold nanoparticles

Olusola B. Adewale[a,b,*], Scholastica O. Anadozie[a,b], Sotonye S. Potts-Johnson[a], Joan O. Onwuelu[a], Tajudeen O. Obafemi[a], Olukemi A. Osukoya[a], Adewale O. Fadaka[c], Hajierah Davids[b], Saartjie Roux[b]

[a] Department of Chemical Sciences, Biochemistry Program, Afe Babalola University, Ado-Ekiti, P.M.B. 5454, Ado-Ekiti, 360001, Nigeria
[b] Department of Physiology, Nelson Mandela University, P. O. Box 77000, Port Elizabeth, 6031, South Africa
[c] Department of Biotechnology, Faculty of Natural Sciences, University of the Western Cape, Bellville, South Africa

ARTICLE INFO

Article history:
Received 27 June 2020
Received in revised form 29 September 2020
Accepted 14 November 2020

Keywords:
Crassocephalum rubens
Bioactive compounds
Breast cancer
Colorectal cancer
Gold nanoparticles

ABSTRACT

The development of cancer therapies has become difficult due to high metastasis, and lack of tissue selectivity, which in most cases affects normal cells. Demand for anticancer therapy is therefore increasing on daily basis. Gold nanoparticles (AuNPs) have many applications in biomedical field. Biological synthesis of AuNPs using aqueous extract of *Crassocephalum rubens* (AECR) was designed to investigate the *in vitro* anticancer potential. The synthesized AuNPs were characterized by UV–vis spectroscopy, high-resolution transmission electron microscopy, and Fourier transform infrared spectroscopy. The characterization results showed the formation of green AuNPs of wavelength 538 nm, and mostly spherical AuNPs with 20 ± 5 nm size. Significant anticancer activity of the AECR-AuNPs on MCF-7 and Caco-2 cells was noted at higher concentrations (125 and 250 μg/mL) during 24 and at all concentrations tested during 48 h. It can therefore be concluded that AECR leaves can mediate stable AuNPs with anticancer properties.

1. Introduction

Cancer is a disease in which genes responsible for the regulation of cell cycle are compromised [1]. Consequently, the cells keep proliferating and eventually form a growth or tumour which can obstruct blood flow or exert immense pressure on neighbouring tissues, thereby preventing their normal functions. Parts of the tumour can dissociate from the primary tumour and metastasize to another area in the body where a new growth develops [2]. Developing an effective cancer therapy has been challenging due to high rates of metastasis. Chemotherapy is available for cancer treatment, but the major limitation is low specificity, and thereby affecting normal tissue as well [3]. Although surgery is the first line of therapy for certain cancers, such as colon and breast cancers. In some, surgery is not always possible or must still be followed by chemotherapy, to assure the extinction of all tumour cells. Radiation therapy also can damage nearby tissue. There is thus an increasing demand for targeted anticancer therapy with less effect on healthy tissues.

The use of nanotechnology-based cancer therapy may be a solution to deliver high doses of potential chemotherapeutic agents, without leakage during circulation before reaching the tumour site [4]. Gold nanoparticles (AuNPs) have received much attention in biomedical applications because of their unique physicochemical and optical properties [5]. Biological methods of AuNPs synthesis are favoured over the chemical and physical methods owing to several factors, including low toxicity, cost-effectiveness, ease of handling, and eco-friendliness [6].

Synthesis of AuNPs using medicinal plant extracts has several advantages over other biological methods (enzymatic and microbial synthesis), in that it is easy to handle, does not require culturing, and can produce large amounts of stable nanoparticles [7]. Several plants and plant products have reportedly been used for the synthesis of metal nanoparticles. These include: synthesis of silver nanoparticles using aqueous extracts of dried powders of *Allium sativum, Capsicum frutescens* and *Zingiber officinale* plants [8], *Cynara scolymus* leaf extract [9] and aqueous extract of *Phyla dulcis* [10]; the use of Saudi's Dates extract in the synthesis of platinum nanoparticles [11]; synthesis of AuNPs using shell extract

* Corresponding author at: Department of Chemical Sciences, Biochemistry Program, Afe Babalola University, Ado-Ekiti, P.M.B. 5454, Ado-Ekiti, 360001, Nigeria.
E-mail addresses: adewaleob@abuad.edu.ng, s215317041@mandela.ac.za (O.B. Adewale).

https://doi.org/10.1016/j.btre.2020.e00560

of *Chenopodium formosanum* [12], leaf extract of *Annona muricata* [13] and *Sasa borealis* leaf extract [14].

Studies have demonstrated cytotoxicity of medicinal plant-mediated AuNPs against different cancer cells [14–16], this potential could be linked to the naturally-inherent phytochemicals in the plant and the specificity afforded by the AuNPs. The use of AuNPs synthesized by means of medicinal plant extract has two advantages: firstly, that the phytochemicals responsible for its medicinal characteristics may become part of the AuNPs, and secondly, the nanoparticles reside longer in the tumor than medicinal plant extract and therefore will have a superior effect. The leaky walls of blood capillaries in tumors and lack of an effective draining system in most tumors [17] allow nanoparticles to concentrate on tumour site.

Crassocephalum rubens (Juss. ex Jacq.) S. Moore is a traditional leafy vegetable, belonging to plant family Asteraceae. It is an erect herb growing up to about 80 cm in length. It is grown and consumed in the Southwestern part of Nigeria, Yemen, South Africa, and the Islands of the Indian Ocean. In Nigeria, it is called "Ebolo" and "Yoruba bologi". The leaves and stems are consumed in soups and stews in the Southwestern part of Nigeria [18]. *C. rubens* is rich in fiber, carbohydrates, proteins, minerals, and vitamins A, B and C. It is also used in several traditional therapeutics for liver dysfunction, stomach inflammation, ocular and ear aches, burns, leprosy and breast cancer [18].

In this study, AuNPs were synthesized using the aqueous extract of *C. rubens* (AECR) leaves, and their anticancer activities against breast cancer (MCF-7) and colorectal cancer (Caco-2) cells were investigated.

2. Materials and methods

2.1. Chemicals

The following chemicals were used in this study: Dulbecco's Modified Eagle Medium, and heat-inactivated fetal bovine serum (FBS) were purchased from Biowest (France), 5′-Fluorouracil, Fulvestrant, sodium dihydrogen phosphate, disodium hydrogen phosphate and gold (III) chloride trihydrate ($HAuCl_4 \cdot 3H_2O$) were purchased from Sigma-Aldrich, USA. All reagents were of analytical grade.

2.2. Plant material and extraction

Crassocephalum rubens leaves were obtained from the Ora-Igbomina farmland, Osun State, Nigeria. The plant part was authenticated at the Forest Research Institute of Nigeria, Ibadan, Oyo State, Nigeria. A sample was deposited at the Department Herbarium with specimen number FHI 112047. The plants were air-dried for 30 days and ground. The resulting powder was then soaked in either distilled water, absolute ethanol, or ethyl acetate for 24 h, followed by filtration using a cheese cloth, and Whatman filter paper number 1. The leaf extracts were then freeze-dried.

2.2.1. Determination of bioactive compounds in different extracts of Crassocephalum rubens *using gas chromatography-mass spectroscopy*

Gas chromatography-mass spectroscopic (GC–MS) analysis of AECR, ethyl acetate extract of *Crassocephalum rubens* (EAECR) and ethanolic extract of *Crassocephalum rubens* (EECR) leaves was completed using the Shimadzu GC–MS-QP2010 Plus, at 250 °C. The split ratio was 20:0, and the carrier gas was nitrogen at an inlet temperature of 250 °C, with a column flow of 1.61 mL/min. The oven program started at a temperature of 60 °C, which was increased to 250 °C at 7 °C/min. A flame-ionization detection (FID) detector was used at 32 °C, at a hydrogen pressure of 22 psi and compressed air of 35 psi. The identification of compounds from the spectral data was based on the available mass spectral records (NIST08 s. Libraries).

2.2.2. Qualitative phytochemical screening

In the AECR, the presence of compounds such as alkaloids, anthraquinones, saponins, tannin, flavonoids, cardiac glycosides, steroids, xanthropoteic amino acids, anthrocyanidins as well as fat and oils, were confirmed according to a procedure reported by Deepti et al. [19], with some modifications.

2.3. Synthesizing and characterizing biogenic AuNPs using C. rubens

Biogenic synthesis of AuNPs was performed by according to a method described by Mapala and Pattabi [20]. with some modifications. Aqueous extract of *C. rubens* (1 mL, 3.125 mg/mL) was added to 4 mL aqueous solution of tetrachloroauric acid (1 mM) on a hot plate, with continuous stirring, at 50 °C for 20 min. The synthesized nanoparticles were washed twice with distilled water by centrifugation at 12,000 x *g* for 15 min to remove excess and unbound plant material in the reaction mixture. The synthesized biogenic AuNPs were then freeze-dried to obtain a powdered form, and stored at −20 °C.

2.3.1. Characterization of the biosynthesized AuNPS

The ultraviolet-visible (UV–vis) spectroscopic analysis of the AuNPs was performed using the Nanodrop 2000c spectrophotometer (Thermoscientific, USA), to determine the wavelength, stability, and aggregation levels of the NPs. The size and morphology of the synthesized AECR-AuNPs was investigated with high resolution transmission electron microscope (HRTEM) JEOL model 1200 LaB6), and the selected area electron diffraction (SAED) analysis was performed to investigate the crystalline nature of the nanoparticles. The Fourier transform infrared (FT-IR) spectroscopy was performed on a dried pellet of AuNPs, to detect the presence of functional groups on the synthesized AuNPs as described by Ghosh et al. [21].

2.4. 1,1-Diphenyl-2-picryl-hydrazyl (DPPH) radical scavenging assay

The radical scavenging activity of AECR and AECR-AuNPs was performed using the DPPH assay, according to a method by Shirwaikar et al. [22], with some modifications. Two mL each of AECR, AECR-AuNPs or quercetin (standard) was added to 2 mL 0.1 mM $DPPH^{\bullet}$ (in methanol). An equal volume of $DPPH^{\bullet}$ and methanol served as a control. The mixture was incubated in the dark at 30 °C for 20 min, and the absorbance read at 517 nm. The DPPH radical scavenging activity of the samples was calculated as follows:

% DPPH radical scavenging activity = ((Abs of control – Abs of sample) / Abs of control) x 100

2.5. Reducing power assay

The reducing power assay was carried out according to a method described by Oyaizu [23]. Each sample (2.5 mL) was mixed with 2.5 mL sodium phosphate buffer (0.2 M) and 2.5 mL potassium ferricyanide (1%), and the mixture was incubated at 50 °C for 20 min. Then, 2.5 mL trichloroacetic acid solution (100 mg/L) was added and the mixture was centrifuged at 1000 x *g* for 10 min. The supernatant (5 mL) was mixed with 5 mL distilled water and 1 mL 0.1 % ferric chloride solution, and the absorbance was read at 700 nm against blank. The reducing power was calculated from a standard curve obtained using varying concentrations of quercetin (0.2–1 mg/mL), and the results presented in mg quercetin equivalent per g extract.

2.6. Anticancer activity of AECR-AuNPs

Cells were obtained from the American Tissue Culture Collection (ATCC). MCF-7 or Caco-2 cells were grown routinely in Dulbecco's Modified Eagle Medium (DMEM), supplemented with 10 % heat-inactivated fetal bovine serum (FBS), 100 μg/mL penicillin and 10 μg/mL streptomycin (Hyclone, Logan, UT) at 37 °C, in a humidified atmosphere with 5% CO_2. The cell viability assay using the tetrazolium dye, 3-[4,5-dimethyl-thiazole-2-yl]-2,5-diphenyl tetrazolium bromide (MTT) assay as described by Mosmann [24], with a slight modification in incubation time, was used to investigate the cytotoxic activity of *C. rubens* leaf extract-mediated AuNPs on MCF-7 and Caco-2 cells. The cells were seeded at a density of 1.25×10^4 cells/100 μL/well in a 96-well plate. Cells were treated with 100 μL AECR-AuNPs (in 0.1 % dimethyl sulfoxide (DMSO)), at 31.25, 62.5, 125 and 250 μg/mL, and standard drugs (5′-Fluorouracil (100 μM) for Caco-2 and Fulvestrant (0.12 μM) for MCF-7). All cell experiments were performed in triplicates.

The cell viability was expressed as follows:

% viability = As/Ac x 100, where As and Ac are the mean absorbance of AECR-AuNPs treated cells and control cells, respectively.

2.7. Cellular morphology of cells treated with AECR-AuNPs

The cellular morphological changes of MCF-7 and Caco-2 cells treated with AECR-AuNPs at 24 were examined using an inverted light microscope. The cells were grown in a 12-well culture plate to 70 % confluence for 24 h, and the spent media was removed from each well. The cells were then treated with the highest concentration of AECR-AuNPs (250 μg/mL) or with positive controls. DMSO (0.1 %) was used as vehicle control for both cells. Cell morphology of both cell lines was examined at 24 h treatment with AECR-AuNPs for possible morphological changes. The cells images were taken at x20 magnification on an inverted light microscope (ZEISS Axio Vert.A1, USA).

2.8. Statistical analysis

Where applicable, results were analyzed using the One-way analysis of variance (ANOVA), using SPSS software package for Windows. Values are presented as Mean ± SD. Intergroup comparison was analyzed using Tukey's test. p values < 0.05 were considered statistically significant.

Table 1
Compounds identified in aqueous extract of *C. rubens* by GC–MS analysis.

No.	R/T (min)	Name of Compound	Area (%)	M/F	M/W (g/mol)
1	3.056	Methoxy-phenyl-oxime	2.48	$C_8H_9NO_2$	151
2	6.299	p-Methoxybenzaldehyde	2.98	$C_8H_8O_2$	136
3	7.118	2-Methyl-3,5-diethylpyrazine	0.17	$C_9H_{14}N_2$	150
4	13.661	Phthalic acid, cyclobutyl tridecyl ester	1.22	$C_{25}H_{38}O_4$	402
5	14.492	2,2-Dimethyl-propyl 2,2-dimethyl-propanesulfinyl sulfone	0.41	$C_{10}H_{22}O_3S_2$	254
6	15.106	1-Iodohexadecane	31.19	$C_{16}H_{33}I$	352
7	15.913	1,2,3-Trimethyldiaziridine	1.70	$C_4H_{10}N_2$	86
8	16.661	2-Bromotetradecane	38.89	$C_{14}H_{29}Br$	276
9	17.431	2-Ethyl-2-methyl-tridecanol	14.50	$Cl_{16}H_{34}O$	242
10	17.674	1-Iodo-Decane	2.66	$C_{10}H_{21}I$	268
11	17.834	2,6,10,14,18-Pentamethyl-2,6,10,14,18-eicosapentaene	3.80	$C_{25}H_{42}$	342

GM-MS analysis of AECR revealed the presence of eleven (11) compounds, with their respective abundance (area), molecular formulae and weights.
M/F – Molecular formula, M/W – Molecular weight, R/T – Retention time.

Table 2
Compounds identified in ethyl acetate extract of *C. rubens* by GC–MS analysis.

No.	R/T (min)	Name of Compound	Area (%)	M/F	M/W (g/mol)
1	3.097	3-Hepten-2-one	1.31	$C_7H_{12}O$	112
2	3.242	3-Ethoxypentane	6.21	$C_7H_{16}O$	116
3	3.532	1,1-Dimethylcyclopentane	11.45	C_7H_{14}	98
4	3.584	2-Ethyl-2-hexenal	6.43	$C_8H_{14}O$	126
5	3.683	2-Oxopentanedioic acid	20.47	$C_5H_6O_5$	146
6	3.829	2-Trimethylsilyloxy-1,3-butadiene	1.66	$C_7H_{14}OSi$	142
7	4.113	Butanal	1.20	C_4H_8O	72
8	4.256	1-(3,4-Methylenedioxybenzylidene)semicarbazide	0.84	$C_9H_9N_3O_3$	207
9	4.735	(Z)-2-Buten-1-ol	1.00	C_4H_8O	72
10	4.781	([(E)-2-Cyclopropylethenyl]oxy)(trimethyl)silane	1.93	$C_8H_{16}OSi$	156
11	8.024	4,4-Dimethyl-8-methylene-2-propyl-1-oxaspiro[2.5]octane	1.28	$C_{13}H_{22}O$	194
12	9.029	1,1-Dimethylethylamine	0.26	$C_4H_{11}N$	73
13	12.775	1,1-Dimethyl-2-propynyl ethyl ether	0.11	$C_7H_{12}O$	112
14	13.125	1,1-Dimethylethylamine	0.22	$C_4H_{11}N$	73
15	13.285	1,1-Dimethyl-2-propynyl ethyl ether	1.25	$C_7H_{12}O$	112
16	13.662	2,3-Hexanediol	1.31	$C_6H_{14}O_2$	118
17	14.163	2,3-Tetramethyleneaziridine	0.74	$C_6H_{11}N$	97
18	14.599	4-Ethylformanilide	1.02	$C_9H_{11}NO$	149
19	14.659	Methyl butyrate	0.38	$C_5H_{10}O_2$	102
20	15.909	2-Acetylisoxazolidine	37.92	$C_5H_9NO_2$	115
21	16.001	4-Ethylformanilide	0.90	$C_9H_{11}NO$	149
22	17.184	2,3-Hexanediol	2.10	$C_6H_{14}O_2$	118

GM-MS analysis of EAECR revealed the presence of twenty-two (22) compounds, with their respective abundance (area), molecular formulae and weights.
M/F – Molecular formula, M/W – Molecular weight, R/T – Retention time.

Table 3
Compounds identified in ethanolic extract of *C. rubens* by GC–MS analysis.

No.	R/T (min)	Name of Compound	Area (%)	M/F	M/W (g/mol)
1	3.070	3-Hepten-2-one	2.78	$C_7H_{12}O$	112
2	3.252	3-Ethoxypentane	4.36	$C_7H_{16}O$	116
3	3.507	3,4-Dimethy-1-pentanol	7.57	$C_7H_{16}O$	116
4	3.690	2-Ethyl-2-hexenal	14.62	$C_8H_{14}O$	126
5	3.835	1,1-Dibutylhydrazine	1.36	$C_8H_{20}N_2$	144
6	4.118	2-Trimethylsilyloxy-1,3-butadiene	0.87	$C_7H_{14}OSi$	142
7	4.260	Butanal	0.77	C_4H_8O	72
8	4.739	([(E)-2-Cyclopropylethenyl]oxy)(trimethyl)silane	0.70	$C_8H_{16}OSi$	156
9	9.025	2-Methyl-2-propanamine	0.30	$C_4H_{11}N$	73
10	13.284	6-Octen-1-ol, 3,7-dimethyl-, propanoate	1.68	$C_{13}H_{24}O_2$	212
11	13.662	4-Ethylformanilide	0.76	$C_9H_{11}NO$	149
12	14.162	Methyl butyrate	0.49	$C_5H_{10}O_2$	102
13	14.809	Methyl 2-methylundecanoate	1.30	$C_{13}H_{26}O_2$	214
14	15.908	Phytol	50.05	$C_{20}H_{40}O$	296
15	16.379	4-methyl-1,4-heptadiene	1.60	C_8H_{14}	110
16	16.379	Diethyl(decyloxy) borane	9.36	$C_{14}H_{31}BO$	226
17	16.767	Oxalic acid, allyl butyl ester	0.31	$C_9H_{14}O_4$	186
18	17.537	Oxalic acid, allyl butyl ester	1.13	$C_9H_{14}O_4$	186

GM-MS analysis of EECR revealed the presence of eighteen (18) compounds, with their respective abundance (area), molecular formulae and weights.
M/F – Molecular formula, M/W – Molecular weight, R/T – Retention time.

Table 4
Qualitative phytochemical screening of aqueous extracts of *C. rubens*.

Test	Result
Alkaloids	++
Anthraquinones	++
Tannins	–
Saponins	++
Flavonoids	++
Polyphenols	+
Cardiac glycosides	++
Steroids	++
Xanthroproteic amino acids	++
Anthrocyanidins	++
Fats and oils	++

In AECR, ++ indicates the presence of the phytochemical, + indicates that the phytochemical is moderately present, and – indicates the absence of the phytochemical.

3. Results

3.1. Bioactive compounds in the aqueous extract of Crassocephalum rubens using GC–MS

analysis of AECR, EAECR and EECR revealed the presence of bioactive compounds. The peaks with their identified bioactive compounds, retention time (RT), molecular weight (M/W), molecular formula (M/F) and area (%) is presented in Tables 1–3, respectively.

3.2. Qualitative phytochemical screening of aqueous extract of Crassocephalum rubens

From the results depicted in Table 4, polyphenols were moderately present; alkaloids, anthraquinones, saponins, flavonoids, cardiac glycosides, steroids, xanthropoteic amino acids, anthrocyanidins and fat and oils were present, while tannins were absent. Only AECR was considered, because as an edible vegetable, water is generally being used in preparation for consumption.

3.3. Synthesis and characterization of biosynthesized gold nanoparticles

Aqueous, ethanolic and ethyl acetate extracts of *C. rubens* leaves were used in the synthesis of AuNPs, with only the AECR suited for the production of AuNPs. The change from the initial dark green colour of AECR to purple of AECR-AuNPs was observed within 20 min, and the nanoparticles (AECR-AuNPs) were without agglomeration when left for a period of one month at room temperature. The UV–vis spectroscopy indicates the maximum absorbance peak at 538 nm for the AECR-AuNPs.

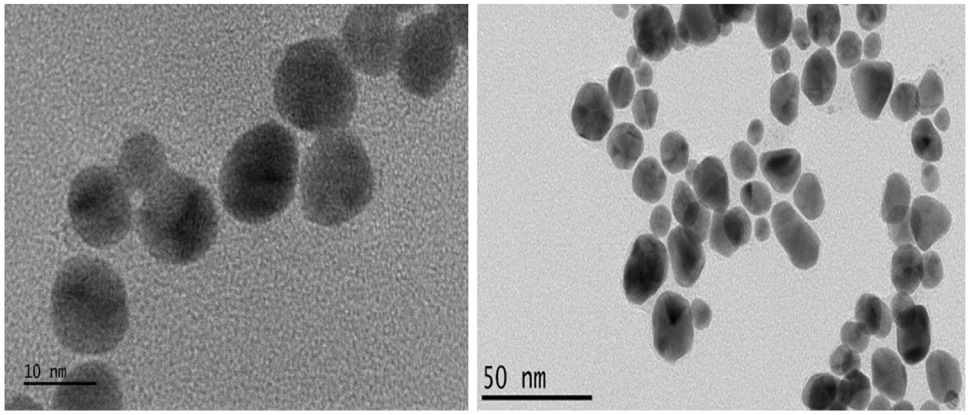

Fig. 1. HRTEM micrograph of AECR-AuNPs. The size (20 ± 5 nm) and shape (mostly spherical) of AECR-AuNPps was assessed using the HRTEM at magnifications of: *x* 10 nm and *x* 50 nm.

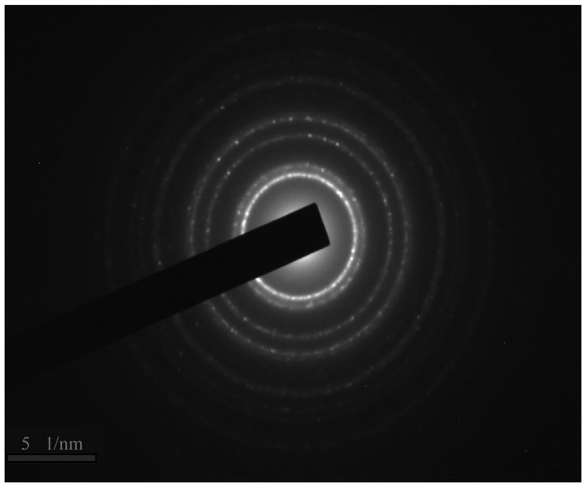

Fig. 2. The selected area electron diffraction (SAED) pattern of the AECR-AuNPs. The SAED result analysis showing the diffraction ring (from inner to outer) corresponding to (111), (200), (220), (311), and (222) reflections of face centered cubic (fcc) crystal phases of gold.

Spherically-shaped AECR-AuNPs, with an average diameter of 20 ± 5 nm, were obtained (Fig. 1), as shown by the TEM. The SAED result analysis (Fig. 2) showed that the diffraction ring corresponding to (111), (200), (220), (311), and (222) reflections of face centered cubic (fcc) crystal phases of gold.

The FT-IR spectra of the AECR and AECR-AuNPs were recorded in the frequency range between 4000 and 450 cm^{-1} in the % transmittance (%T) mode (Fig. 3). Broad peaks were noted at 3281.03, 1632.93, 1518.78, 1447.46, 1264.76, 1164.7, 1131.55, 1083.26 cm^{-1} for AECR-AuNPs, and 3350.83, 1638.58, 1400.22, 1220.16, 1080.85, 912.37, 533.64, and 466.55 cm^{-1} for the AECR. Similar compounds were present in the spectra of both AECR-AuNPs and AECR, however a slight shift was noted in the AECR-AuNPs peaks when compared to the AECR. The 3350.83 cm^{-1} band peak in the FTIR spectra corresponds to O—H stretch in AECR which shifted to 3281.03 cm^{-1} in the AECR-AuNPs. The 1447.46, 1264.76 and 1164.76 cm^{-1} of AECR-AuNPs and 1400.22, 1220.16 and 1080.85 cm^{-1} of AECR corresponds to the characteristics of C–H, C=C and C—O stretching vibrations, respectively.

3.4. In vitro *antioxidant potential and reducing power capabilities of AECR and AECR-AuNPs*

Significant differences ($p < 0.05$) in the % inhibition of DPPH radical were noted in the AECR and AECR-AuNPs when compared to quercetin at higher concentrations (2–5 mg/mL), but no significant difference was noted in AECR-AuNPs when compared to the AECR (Fig. 4). At lower concentration (1 mg/mL), no significant difference was noted in AECR and AECR-AuNPs when compared to quercetin. The reducing power of AECR and AECR-AuNPs were 110.62 ± 18.53 and 86.31 ± 13.18 mg quercetin equivalent/g sample, respectively.

3.5. Anticancer activity of AECR-AuNPs on breast cancer cells

The anticancer activity of AECR-AuNPs on breast cancer (MCF-7) cells is shown in Fig. 5. Significant ($p < 0.05$) cytotoxicity in MCF-7 cells was noted when exposed to fulvestrant and AECR-AuNPs, at all concentrations tested, when compared to the vehicle control at 24 and 48 h. At lower concentrations (31.25 and 62.50 μg/mL), % viability of cells was significantly increased ($p < 0.05$) at 24 h, the AECR-AuNPs at all concentrations were as cytotoxic as the positive control at 48 h. At both 24 and 48 h, the 125 and 250 μg/mL AECR-AuNPs were also as cytotoxic as the positive control.

3.6. Cytotoxic effect of AECR-AuNPs on colorectal cancer cells

Fig. 6 indicates the cytotoxicity of AECR-AuNPs on colorectal cancer (Caco-2) cells. At 24 h, the % viability of cells treated with AECR-AuNPs were significantly increased and decreased ($p < 0.05$) when compared to 5′-Flurouracil and the vehicle control, respectively, at all concentrations tested. It was noted that higher concentrations (125 and 250 μg/mL) of AECR-AuNPs were cytotoxic, with less than 50 % cell viabilities. However, at 48 h, there were no significant differences ($p > 0.05$) in the % cell viability of cells treated with higher concentrations of AECR-AuNPs (62.5, 125 and 250 μg/mL) when compared to the 5′-Flurouracil. A significant decrease ($p < 0.05$) in the % cell viability was observed in cells treated with all tested concentrations of AECR-AuNPs, as well as 5′-Flurouracil when compared to the vehicle control.

3.7. Effect of AECR-AuNPs on cellular morphology

Fig. 7 and 8 shows the effect of AECR-AuNPs on the cellular morphology of both MCF-7 and Caco-2 cells. Cellular/structural changes were observed in MCF-7 and Caco-2 cells at 24 h treatment with the positive controls (Fulvestrant and 5′- Fluorouracil) and AECR-AuNPs. The vehicle control cells maintained their membrane integrity without visible changes in the cell morphology. Changes in the cell morphology was observed in both cell lines after 24 h of AECR-AuNPs treatment. The MCF-7 cells at 24 h exhibited apoptotic features such as cell shrinkage and membrane blebbing, while Caco-2 cells were rounding up and detaching from the plate. The morphological changes observed when both cell lines were treated with 250 μg/mL AECR-AuNPs were similar to the changes noted with the positive controls.

4. Discussion

Herbal medicine involves the use of plants and plant products in the treatment of various ailments caused by free radical generation [25]. *C. rubens*, in combination with *C. crepidioides*, contain several medicinal activities, which include antibiotic, anti-diabetic, anti-helminthic, anti-inflammatory, anti-malarial, and blood regulation properties [26]. The use of *C. rubens* locally in the treatment of breast cancer [18,27], and basal diets fortified with the leaf in the chemoprevention of colorectal cancer in rats [28], have been reported. These properties could be linked to secondary compounds inherent in the plant. Polyphenols present in plants and plant products are secondary metabolites, and have been reported to demonstrate pharmacological effects which could be related to their antioxidant potential [29].

Cancer is one of the major global health problems. Breast cancer is the most common cancer among women, while colorectal cancer is among the leading type of cancer and cause of cancer-related deaths, globally [30]. Various therapeutic approaches are in use for these types of cancers. Cancer therapy of plant origin is at the forefront due to naturally inherent compounds that are readily available, less toxic, and cost-effective. Compounds, including saponins, phenols, and glycosides have reportedly been used in chemotherapy [31]. Qualitative phytochemical screening of this study (Table 4) confirmed the presence of these compounds in *C. rubens* and is similar to the findings of Ojo and Adenegan-Alakinde [18], except the absence of tannins, which may be due to extraction solvent (alcohol) they used.

Different phytochemicals noted with GC–MS analysis of the different extractions of *C. rubens* (Tables 1–3), indicate the role of solvent in the extraction of bioactive compounds from plants [32].

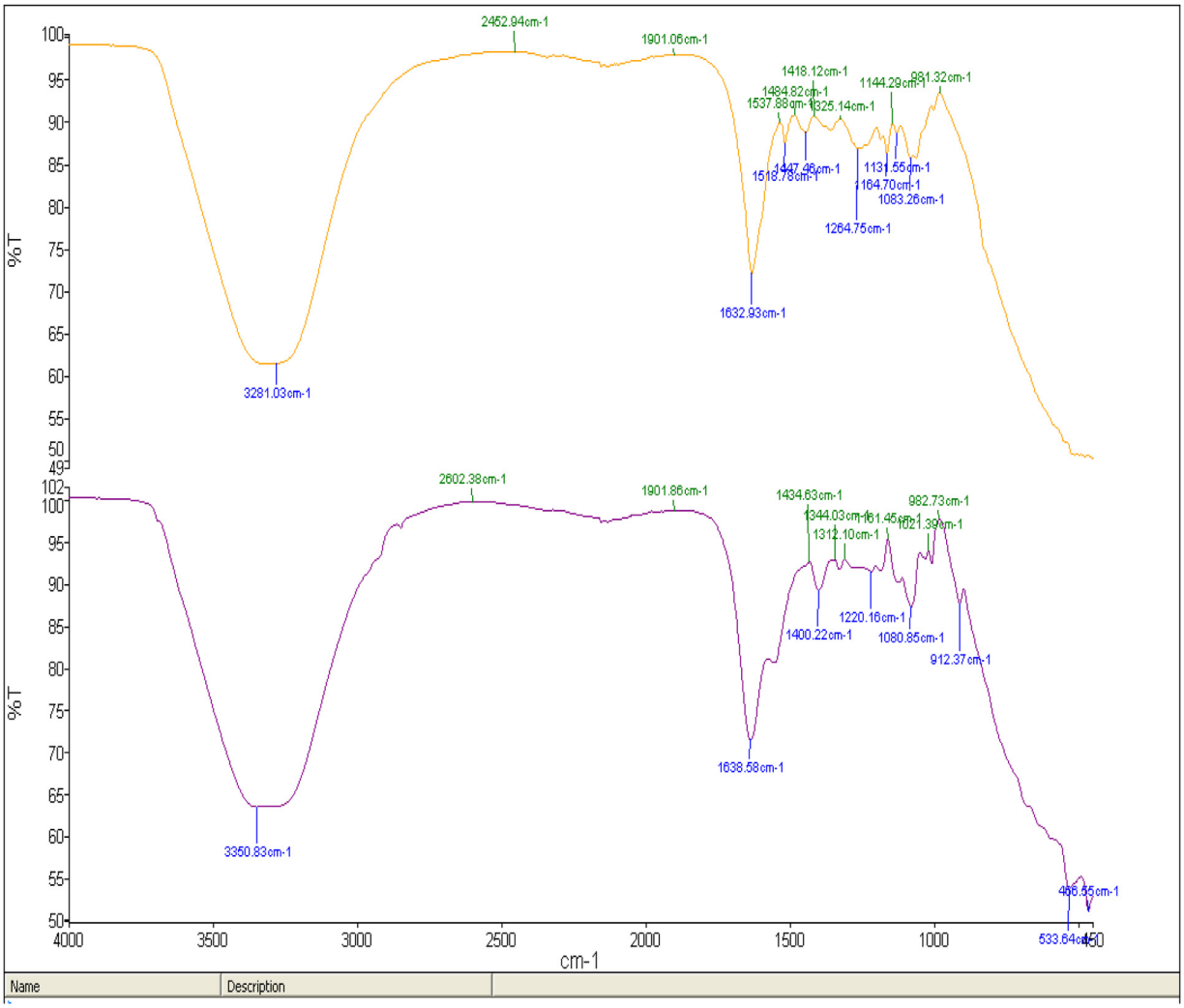

Fig. 3. FT-IR spectra of AECR AND AECR-AuNPs. The various functional groups in AECR-AuNPs (above spectra, in orange) was compared with AECR (below spectra, in purple) using the FT-IR spectroscopic analysis.

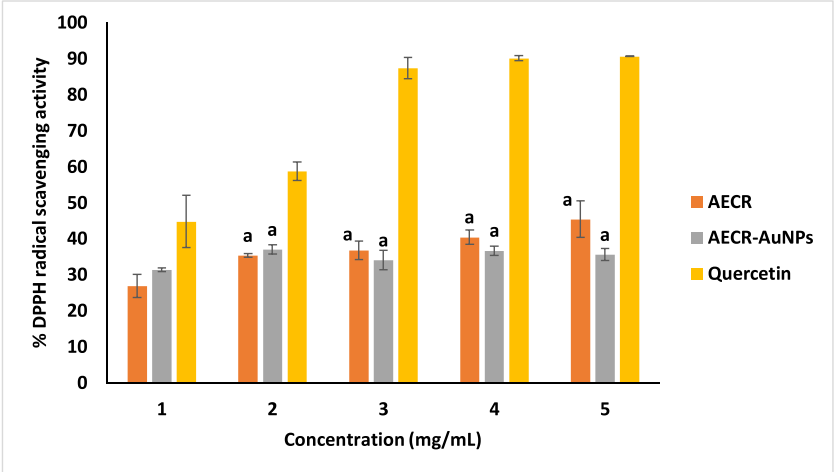

Fig. 4. DPPH scavenging activities of AECR and AECR-AuNPs at various concentrations. The antioxidant potential of aqueous extract of *Crassocephalum rubens* (AECR) and the corresponding gold nanoparticles (AECR-AuNPs), at different concentrations, were assessed using the DPPH radical scarvenging assay.
Each data is presented as mean ± SD (n = 3). [a]$p < 0.05$ compared to quercetin.

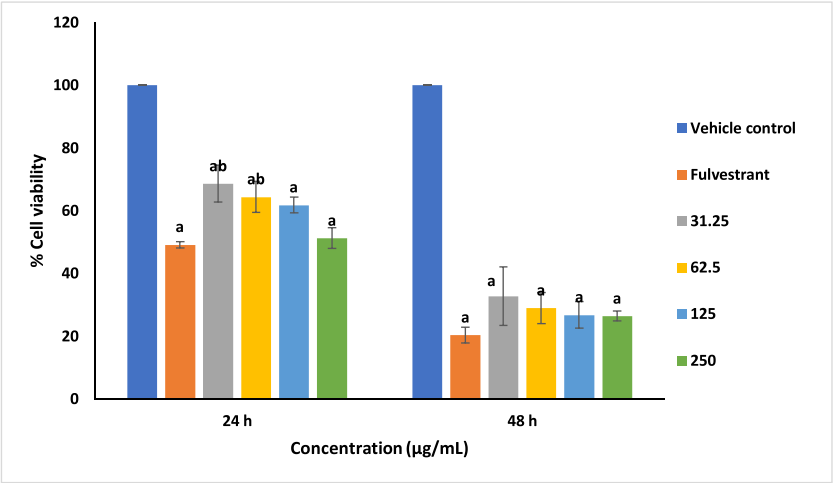

Fig. 5. Cytotoxicity of AECR-AuNPs in breast cancer (MCF-7) cells. Percentage viability of MCF-7 cells was assessed using the MTT assay after 24 and 48 h incubation with increasing concentrations of AECR-AuNPs.
Each data is presented as mean ± SD (n = 3). [a]$p < 0.05$ compared to the vehicle control, [b]$p < 0.05$ compared to Fulvestrant (0.12 µM).

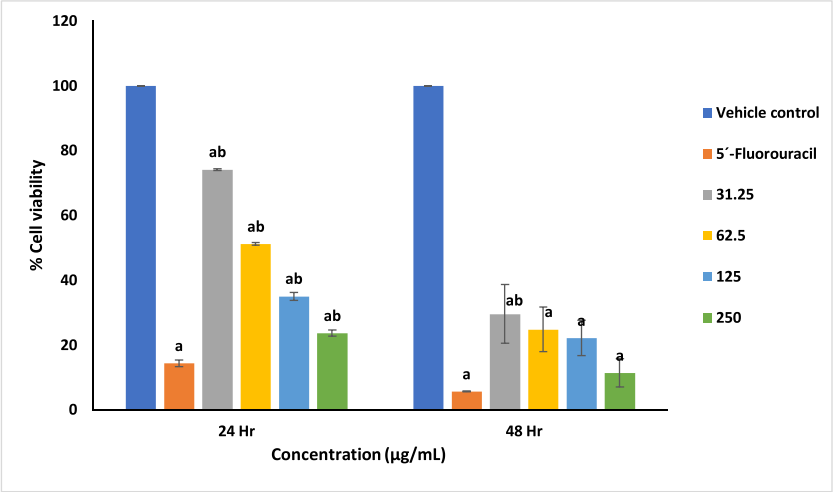

Fig. 6. Cytotoxicity of AECR-AuNPs in colorectal cancer (Caco-2) cells. Percentage viability of Caco-2 cells was assessed using the MTT assay, after 24 and 48 h incubation with increasing concentrations of AECR-AuNPs.
Each data is presented as mean ± SD (n = 3). [a]$p < 0.05$ compared to the control group, [b]$p < 0.05$ compared to 5-Fluorouracil (100 µM).

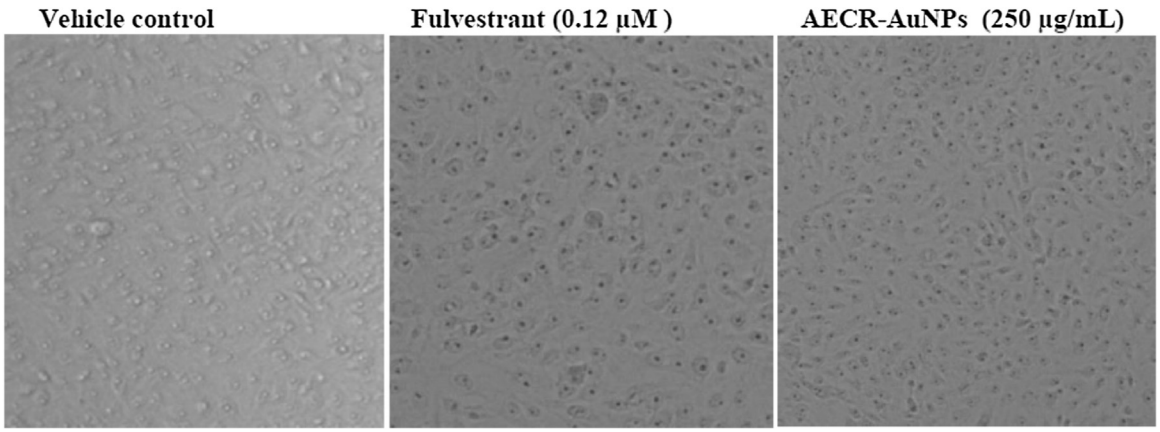

Fig. 7. Representative photomicrograph of MCF-7 cells under bright light microscope showing cell morphology. Cells were treated with Fulvestrant and highest concentration of AECR-AuNPs (250 µg/mL). Vehicle control (0.1 % DMSO).
Magnification was taken at × 40.

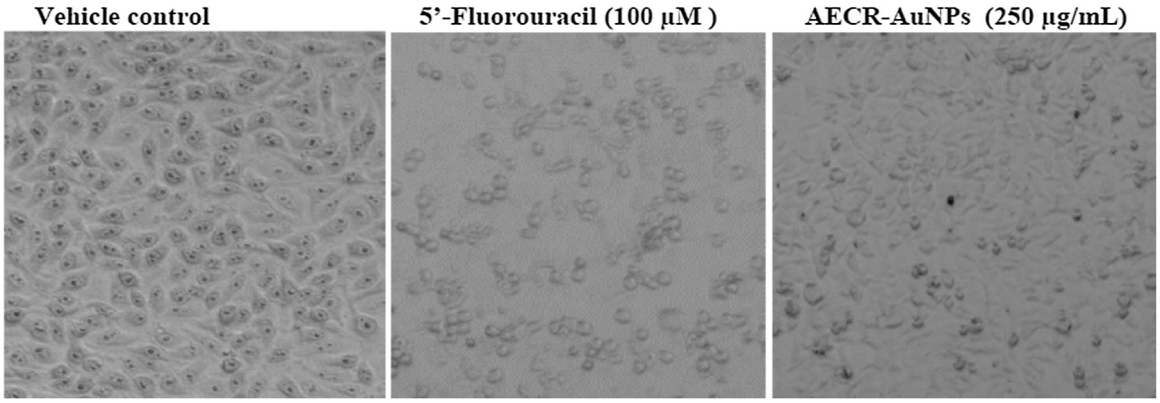

Fig. 8. Representative photomicrograph of Caco-2 cells under bright light microscope showing cell morphology. Cells were treated with 5′-Fluorouracil and highest concentration of AECR-AuNPs (250 µg/mL). Vehicle control (0.1 % DMSO).
Magnification was taken at × 40.

The aqueous (traditional medium of preparation) extract of *C. rubens* was used in the synthesis of AuNPs in this study, as it produced the most stable AuNPs. The use of EECR and EAECR in the synthesis of stable AuNPs is underway, as the reason for the aggregation is currently unknown.

The colour change noted during the biosynthesis of AuNPs using AECR indicated a reduction of the synthetic process [33], with the inherent phytochemicals in plants (*C. rubens*) were responsible for the stability [34], by providing a coating on the surface of the AuNPs. The formation and stability of the nanoparticles was confirmed by UV–vis spectroscopy, of which the AECR-AuNPs were found in the wavelength range of 500−600 nm, a typical surface plasmon resonance (SPR) of AuNPs [35–37]. The mostly spherical shapes of the AECR-AuNPs, as demonstrated by the HRTEM (Fig.1) indicates that the nanoparticles were polydispersed in nature. This could be due to the presence of more than one reducing agent (phytochemicals) in the *C. rubens* leaf extract. This was confirmed by the GC–MS results, indicating the presence of several compounds in extracts of *C. rubens* (Tables 1–3). The bright circular rings observed in the SAED patterns (Fig. 2) indicate that the synthesized AuNPs are polycrystalline in nature, which can be linked to the fcc structure of gold [38].

In the FT-IR analysis (Fig. 3), the slight shifts noted in broad peaks at 3350.83 cm^{-1} for AECR and 3281.03 cm^{-1} for AECR-AuNPs, indicate the presence of the O—H stretch for alcohol or phenol. Also, the 1632.93 cm^{-1} and 1638.58 cm^{-1} for AECR-AuNPs and AECR, respectively, corresponded to C—O and N—H stretching and bending for carboxylic acids and amides. This suggests that polyphenolic compounds and proteins were involved in the synthesis of AuNPs through the reduction of gold salt to AuNPs. Phenolic compounds reportedly have excellent binding affinity to metal ions, thereby aiding the reduction of gold ions (Au^{3+}) to gold atoms and induce chelation effect [39]. The presence of carboxylate groups on proteins serve as surfactant for the synthesis of nanoparticles, thereby enabling excellent affinity of the proteins for AuNPs [40]. These prevents the aggregation of the nanoparticles [39,40].

Antioxidant and free radical scavenging activity studies of plants and plant products are essential to investigate their role against toxic effects of free radicals in biological systems. Free radicals readily bind and oxidize biomolecules, including carbohydrates, lipids and proteins, resulting in tissue damage, cellular death, and various diseases including inflammation and cancer [41]. The methanolic extract of *C. rubens* leaves have been screened for its DPPH radical scavenging, reducing power and total antioxidant properties [42], where the antioxidant activity was associated with the ability of the plant to scavenge highly reactive free radicals. This was also observed in the present study (Fig. 4).

To enhance cancer specificity and targeted therapy, AuNPs were synthesized using AECR. The non-significant difference noted in the antioxidant and reducing potential result of AECR compared to that of AECR-AuNPs suggests the presence of phytochemicals capping the AuNPs. It is expected based on these parameters that AECR-AuNPs possess the ability to scavenge free radicals, mostly at lower concentrations, which could serve as potential anti-inflammatory and anticancer agent. In view of this, the cytotoxic effect of AECR-AuNPs was investigated against breast and colorectal cancer cells.

The MTT assay is an *in vitro* model used to measure the cytotoxic effect of substances against several cancer cell lines [43–46]. The anticancer potential of AECR-AuNPs noted in our study, as shown in Fig. 5 and 6, further suggests the use of *C. rubens* synthesized nanoparticles in breast and colorectal cancer therapy. This supports the findings of Alhassan and Atawodi [28] on the chemopreventive potential of *C. rubens* leaf fortified diet against N-methyl-N-nitrosourea induced colorectal cancer in rats. The *in vitro* cytotoxicity of the AECR-AuNPs against breast cancer (MCF-7) and colorectal cancer (Caco-2) cells were more evidenced at higher concentrations (125 and 250 µg/mL) at 24 h, and at all concentrations tested at 48 h (Fig. 5 and 6). The AECR-AuNPs was however more sensitive to the Caco-2 cells than the MCF-7 both at 24 and 48 h. In comparing the effect of AECR-AuNPs to the standard drugs (Fulvestrant and 5- Fluorouracil) used for both cell lines, the AECR-AuNPs showed good cytotoxic activities, and thus can be used as possible anti-cancer agent. The enhanced cytotoxic effect of AECR-AuNPs against MCF-7 and Caco-2 cells could be due to the presence of phytochemicals on the surface of the AECR-AuNPs, and the small size of the AuNPs which aids their uptake by the cells.

To confirm the cytotoxic effect of the AECR-AuNPs on both cell lines as demonstrated in the MTT viability assay, the cellular morphology was investigated using an inverted light microscope. Plant synthesized gold nanoparticles have been reported to induce cancer cell death by means of apoptotic properties including membrane blebbing, cell shrinkage and morphology changes and chromatin condensation [47–49]. The intact membrane structure for vehicle control cells of both MCF-7 and Caco-2 at 24 h suggests no cellular death. Cellular changes observed in the cells treated with AECR-AuNPs at 24 h (Fig. 7 and 8) indicates that the treatment is cytotoxic to the cells. These changes were however more pronounced in the Caco-2 cells at 24 h. This confirms the MTT cytotoxicity results where treatment with AECR-AuNPs was more sensitive to Caco-2 cells. The cytotoxic effect of AECR-AuNPs on MCF-7 and Caco-2 cells, as demonstrated by changes in the cell

morphology, suggest that the AECR-AuNPs can be used as possible therapeutic agent for both breast and colorectal cancers.

5. Conclusion

It can therefore be concluded that *C. rubens* leaf contains a wide range of secondary metabolites, which could be responsible for the reduction of gold ions to AuNPs, and thus responsible for the biological synthesis of AuNPs. This further reveals the use of AECR-mediated AuNPs as a potential anticancer agent. *in vivo* studies are underway to provide more information on the targeted anticancer potential of AECR-AuNPs and the mechanism of action of this tool.

CRediT authorship contribution statement

Olusola B. Adewale: Conceptualization, Formal analysis, Methodology, Project administration, Supervision, Validation, Visualization, Writing - original draft. **Scholastica O. Anadozie:** Data curation, Formal analysis, Methodology, Software, Investigation. **Sotonye S. Potts-Johnson:** Data curation, Funding acquisition, Investigation. **Joan O. Onwuelu:** Data curation, Funding acquisition, Investigation. **Tajudeen O. Obafemi:** Resources, Writing - review & editing. **Olukemi A. Osukoya:** Resources, Writing - review & editing. **Adewale O. Fadaka:** Software, Validation, Writing - review & editing. **Hajierah Davids:** Resources, Writing - review & editing. **Saartjie Roux:** Resources, Writing - review & editing.

Declaration of Competing Interest

The authors report no declarations of interest.

Acknowledgments

This research did not receive any specific grant from funding agencies in the public, commercial, or not-for-profit sectors. The authors acknowledge technical assistance from Mr Johnson Jonathan of the Department of Chemical Sciences, Afe Babalola University, Ado-Ekiti, Nigeria.

Appendix A. Supplementary data

Supplementary material related to this article can be found, in the online version, at doi:https://doi.org/10.1016/j.btre.2020.e00560.

References

[1] A. Minami, T. Murai, A. Nakanishi, et al., Cell cycle regulation via the p53, PTEN, and BRCA1 tumor suppressors, in: D. Bulgin (Ed.), New Aspects in Molecular and Cellular Mechanisms of Human Carcinogenesis, IntechOpen, 2016.
[2] T.N. Seyfried, L.C. Huysentruyt, On the origin of cancer metastasis, Crit. Rev. Oncogen. 18 (2013) 43–73, doi:http://dx.doi.org/10.1615/critrevoncog.v18.i1-2.40.
[3] Q. Gao, G. Zhou, S.-J. Lin, et al., How chemotherapy and radiotherapy damage the tissue: comparative biology lessons from feather and hair models, Exp. Dermatol. 28 (2019) 413–418, doi:http://dx.doi.org/10.1111/exd.13846.
[4] K. Sowjanya, A review on current advancements in nanotechnology, Res. Rev.: J. Med. Health Sci. 4 (2015).
[5] Y.P. Jia, B.Y. Ma, X.W. Wei, et al., The in vitro and in vivo toxicity of gold nanoparticles, Chin. Chem. Lett. 28 (2017) 691–702, doi:http://dx.doi.org/10.1016/j.cclet.2017.01.021.
[6] O.B. Adewale, H. Davids, L. Cairncross, et al., Toxicological behavior of gold nanoparticles on various models: influence of physicochemical properties and other factors, Int. J. Toxicol. 38 (2019) 357–384, doi:http://dx.doi.org/10.1177/1091581819863130.
[7] A. Tripathi, S. Kumari, A. Kumar, Toxicity evaluation of pH dependent stable Achyranthes aspera herbal gold nanoparticles, Appl. Nanosci. 6 (2016) 61–69, doi:http://dx.doi.org/10.1007/s13204-015-0414-x.
[8] M. Reda, A. Ashames, Z. Edis, et al., Green synthesis of potent antimicrobial silver nanoparticles using different plant extracts and their mixtures, Processes 7 (2019), doi:http://dx.doi.org/10.3390/pr7080510.
[9] O. Erdogan, M. Abbak, G.M. Demirbolat, et al., Green synthesis of silver nanoparticles via Cynara scolymus leaf extracts: the characterization, anticancer potential with photodynamic therapy in MCF7 cells, PLoS One 14 (2019)e0216496, doi:http://dx.doi.org/10.1371/journal.pone.0216496.
[10] L. Carson, S. Bandara, M. Joseph, et al., Green synthesis of silver nanoparticles with antimicrobial properties using Phyla dulcis plant extract, Foodborne Pathog. Dis. 17 (2020) 504–511, doi:http://dx.doi.org/10.1089/fpd.2019.2714.
[11] N.S. Al-Radadi, Green synthesis of platinum nanoparticles using Saudi's Dates extract and their usage on the cancer cell treatment, Arab. J. Chem. 12 (2018) 330–349, doi:http://dx.doi.org/10.1016/j.arabjc.2018.05.008.
[12] M.-N. Chen, C.-F. Chan, S.-L. Huang, et al., Green biosynthesis of gold nanoparticles using Chenopodium formosanum shell extract and analysis of the particles' antibacterial properties, J. Sci. Food Agric. 99 (2019) 3693–3702, doi:http://dx.doi.org/10.1002/jsfa.9600.
[13] A. Folorunso, S. Akintelu, A.K. Oyebamiji, et al., Biosynthesis, characterization and antimicrobial activity of gold nanoparticles from leaf extracts of Annona muricata, J. Nanostructure Chem. 9 (2019) 111–117, doi:http://dx.doi.org/10.1007/s40097-019-0301-1.
[14] X. Jin, N.C. Simeon, J. Palma, et al., Anticancer activity of Sasa borealis leaf extract-mediated gold nanoparticles AU - Patil, Maheshkumar Prakash, Artif. Cells Nanomed. Biotechnol. 46 (2018) 82–88, doi:http://dx.doi.org/10.1080/21691401.2017.1293675.
[15] A.C. Barai, K. Paul, A. Dey, et al., Green synthesis of Nerium oleander-conjugated gold nanoparticles and study of its in vitro anticancer activity on MCF-7 cell lines and catalytic activity, Nano Converg. 5 (2018) 10, doi:http://dx.doi.org/10.1186/s40580-018-0142-5.
[16] S. Rajeshkumar, Anticancer activity of eco-friendly gold nanoparticles against lung and liver cancer cells, J. Genet. Eng. Biotechnol. 14 (2016) 195–202, doi:http://dx.doi.org/10.1016/j.jgeb.2016.05.007.
[17] P.R. Gil, W.J. Parak, Composite nanoparticles take aim at cancer, ACS Nano 2 (2008) 2200–2205, doi:http://dx.doi.org/10.1021/nn800716j.
[18] F.M. Ojo, T.A. Adenegan-Alakinde, Phytochemical studies of four indigenous vegetables commonly consumed in ile-ife, South-West Nigeria, Int J Curr Sci. 21 (2017) E6–13.
[19] K. Deepti, P. Umadevi, G. Vijayalakshmi, et al., Antimicrobial activity and phytochemical analysis of Morinda tinctoria Roxb. leaf extracts, Asian Pac. J. Trop. Biomed. 2 (2012) S1440–S1442, doi:http://dx.doi.org/10.1016/S2221-1691(12)60433-X.
[20] K. Mapala, M. Pattabi, Mimosa pudica flower extract mediated green synthesis of gold nanoparticles, NanoWorld J. 03 (2017) 44–50, doi:http://dx.doi.org/10.17756/nwj.2017-045.
[21] S. Ghosh, S. Patil, M. Ahire, et al., Gnidia glauca flower extract mediated synthesis of gold nanoparticles and evaluation of its chemocatalytic potential, J. Nanobiotechnol. 10 (2012) 1–9, doi:http://dx.doi.org/10.1186/1477-3155-10-17.
[22] A. Shirwaikar, A. Shirwaikar, R. Kuppusamy, et al., In vitro antioxidant studies on the Benzyl Tetra Isoquinoline alkaloid berberine, Biol. Pharm. Bull. 29 (2006) 1906–1910, doi:http://dx.doi.org/10.1248/bpb.29.1906.
[23] M. Oyaizu, Studies on products of browning reactions: antioxidative activities of products of browning reaction prepared from glucosamine, Jpn. J. Nutr. Diet. 44 (1986) 307–315.
[24] T. Mosmann, Rapid colorimetric assay for cellular growth and survival: application to proliferation and cytotoxicity assays, J. Immunol. Methods 65 (1983) 55–63, doi:http://dx.doi.org/10.1016/0022-1759(83)90303-4.
[25] H.S. Abou Seif, Physiological changes due to hepatotoxicity and the protective role of some medicinal plants, Beni-Suef Univ. J. Basic Appl. Sci. 5 (2016) 134–146, doi:http://dx.doi.org/10.1016/j.bjbas.2016.03.004.
[26] A. Adjatin, A. Dansi, E. Badoussi, et al., Phytochemical screening and toxicity studies of Crassocephalum rubens (Juss. ex Jacq.) S. Moore and Crassocephalum crepidioides (Benth.) S. Moore consumed as vegetable in Benin, J. Chem. Pharm. Res. 5 (2013) 160–167.
[27] C.H. Bosch, Crassocephalum rubens (Juss. ex Jacq.) S.Moore. [Internet] Record from PROTA4U, in: G.J.H.D. Grubben, O.A (Eds.), PROTA (Plant Resources of Tropical Africa / Ressources végétales de l'Afrique tropicale), Wageningen, Netherlands, 2004.
[28] S.O. Alhassan, S.E.-O. Atawodi, Chemopreventive effect of dietary inclusion with Crassocephalum rubens (Juss ex Jacq) leaf on N-methyl-N-nitrosourea (MNU)-induced colorectal carcinogenesis in Wistar rats, J. Funct. Foods 63 (2019) 103589, doi:http://dx.doi.org/10.1016/j.jff.2019.103589.
[29] O.B. Adewale, A. Onasanya, A.O. Fadaka, et al., In vitro antioxidant effect of aqueous extract of Solanum macrocarpon leaves in rat liver and brain, Oxid. Antioxid. Med. Sci. 3 (2014) 225–229.
[30] F. Bray, J. Ferlay, I. Soerjomataram, et al., Global cancer statistics 2018: GLOBOCAN estimates of incidence and mortality worldwide for 36 cancers in 185 countries, CA Cancer J. Clin. 68 (2018) 394–424, doi:http://dx.doi.org/10.3322/caac.21492.
[31] M. Maqsood, R. Qureshi, M. Ikram, et al., In vitro anticancer activities of Withania coagulans against HeLa, MCF-7, RD, RG2, and INS-1 cancer cells and phytochemical analysis, Integr. Med. Res. 7 (2018) 184–191, doi:http://dx.doi.org/10.1016/j.imr.2018.03.003.
[32] J.F. Cossetin, E. da Silva Brum, R. Casoti, et al., Peanut leaf extract has antioxidant and anti-inflammatory activity but no acute toxic effects, Regul. Toxicol. Pharmacol. 107 (2019) 104407, doi:http://dx.doi.org/10.1016/j.yrtph.2019.104407.
[33] S. Khan, J. Bakht, F. Syed, Green synthesis of gold nanoparticles using Acer pentapomicum leaves extract its characterization, antibacterial, antifungal and antioxidant bioassay, Dig. J. Nanomater. Bios. 2 (2018) 579–589.

[34] A.N. Geraldes, A.A. da Silva, J. Leal, et al., Green nanotechnology from plant extracts: synthesis and characterization of gold nanoparticles, Adv. Nanopart. 5 (2016) 176.
[35] K.O. Shittu, M.T. Bankole, A.S. Abdulkareem, et al., Application of gold nanoparticles for improved drug efficiency, Adv. Nat. Sci.-Nanosci. 8 (2017) 035014, doi:http://dx.doi.org/10.1088/2043-6254/aa7716.
[36] C. Gonnelli, F. Cacioppo, C. Giordano, et al., Cucurbita pepo L. extracts as a versatile hydrotropic source for the synthesis of gold nanoparticles with different shapes, Green Chem. Lett. Rev. 8 (2015) 39–47, doi:http://dx.doi.org/10.1080/17518253.2015.1027288.
[37] P. Singh, S. Pandit, J. Garnæs, et al., Green synthesis of gold and silver nanoparticles from Cannabis sativa (industrial hemp) and their capacity for biofilm inhibition, Int. J. Nanomed. 13 (2018) 3571–3591, doi:http://dx.doi.org/10.2147/ijn.s157958.
[38] R. Vijayakumar, V. Devi, K. Adavallan, et al., Green synthesis and characterization of gold nanoparticles using extract of anti-tumor potent Crocus sativus, Physica E Low. Syst. Nanostruct. 44 (2011) 665–671, doi:http://dx.doi.org/10.1016/j.physe.2011.11.002.
[39] T. Ahmad, M.A. Bustam, M. Irfan, et al., Mechanistic investigation of phytochemicals involved in green synthesis of gold nanoparticles using aqueous Elaeis guineensis leaves extract: role of phenolic compounds and flavonoids, Biotechnol. Appl. Biochem. 66 (2019) 698–708, doi:http://dx.doi.org/10.1002/bab.1787.
[40] K.X. Lee, K. Shameli, Y.P. Yew, et al., Recent developments in the facile bio-synthesis of gold nanoparticles (AuNPs) and their biomedical applications, Int. J. Nanomed. 15 (2020) 275–300, doi:http://dx.doi.org/10.2147/ijn.s233789.
[41] E. Koksal, E. Bursal, E. Dikici, et al., Antioxidant activity of Melissa officinalis leaves, J. Med. Plant Res. 5 (2011) 217–222.
[42] E. Omoregie, A. Osagie, E. Iruolaje, In vitro antioxidant activity and the effect of methanolic extracts of some local plants on nutritionally stressed rats, Pharmacologyonline 1 (2011) 23–56.
[43] I. Turan, S. Demir, K. Kilinc, et al., Cytotoxic effect of Rosa canina extract on human colon cancer cells through repression of telomerase expression, J. Pharm. Anal. 8 (2018) 394–399, doi:http://dx.doi.org/10.1016/j.jpha.2017.12.005.
[44] M. Khatami, I. Sharifi, M.A.L. Nobre, et al., Waste-grass-mediated green synthesis of silver nanoparticles and evaluation of their anticancer, antifungal and antibacterial activity, Green Chem. Lett. Rev. 11 (2018) 125–134, doi:http://dx.doi.org/10.1080/17518253.2018.1444797.
[45] Y. Huo, P. Singh, Y.J. Kim, et al., Biological synthesis of gold and silver chloride nanoparticles by Glycyrrhiza uralensis and in vitro applications, Artif. Cells Nanomed. Biotechnol. 46 (2018) 303–312, doi:http://dx.doi.org/10.1080/21691401.2017.1307213.
[46] A. Alaklabi, I.A. Arif, A. Ahamed, et al., Evaluation of antioxidant and anticancer activities of chemical constituents of the Saururus chinensis root extracts, Saudi J. Biol. Sci. 25 (2018) 1387–1392, doi:http://dx.doi.org/10.1016/j.sjbs.2016.12.021.
[47] F. Namvar, H.S. Rahman, R. Mohamad, et al., Apoptosis induction in human leukemia cell lines by gold nanoparticles synthesized using the green biosynthetic approach, J. Nanomater. 2015 (2015)642621, doi:http://dx.doi.org/10.1155/2015/642621.
[48] V. Ramalingam, S. Revathidevi, T. Shanmuganayagam, et al., Biogenic gold nanoparticles induce cell cycle arrest through oxidative stress and sensitize mitochondrial membranes in A549 lung cancer cells, RSC Adv. 6 (2016) 20598–20608, doi:http://dx.doi.org/10.1039/C5RA26781A.
[49] L. Wang, J. Xu, Y. Yan, et al., Green synthesis of gold nanoparticles from Scutellaria barbata and its anticancer activity in pancreatic cancer cell (PANC-1), Artif. Cells Nanomed. Biotechnol. 47 (2019) 1617–1627, doi:http://dx.doi.org/10.1080/21691401.2019.1594862.